

Compressive mechanical response of a low-density epoxy foam at various strain rates

B. Song · W. Chen · W.-Y. Lu

Received: 13 November 2006 / Accepted: 13 February 2007 / Published online: 18 May 2007
© Springer Science+Business Media, LLC 2007

Abstract We experimentally obtained compressive stress–strain response of a low-density epoxy foam at various strain rates. In particular, compressive stress–strain behavior at intermediate strain rates that has not been previously well understood were characterized by using a modified MTS and a split Hopkinson pressure bar (SHPB). Strain rate effects on the modulus of elasticity and cell-collapse stress for this low-density epoxy foam were determined.

Introduction

Polymeric foams have been recognized to exhibit excellent cushion and energy-absorbing properties such that they have been utilized in a wide range of applications, such as packaging and transportation, the automotive industry, and aerospace components. Among these applications, the foam components are inevitably subjected to a variety of loading conditions from static to impact loadings. Mechanical response of the foam materials at various strain rates is thus desired to be understood and quantified to develop strain-rate-dependent material models for realistic numerical simulations in these applications.

Quasi-static compressive response of polymeric foams is usually investigated with hydraulic testing frames such as Instron and MTS materials testing systems. Under impact loading conditions, the stress–strain behavior characterization has been mostly conducted with split Hopkinson bars which were originally developed by Kolsky in 1949 [1]. In most cases, the strain rates in an Instron or MTS test can be up to 10^{-1} s^{-1} ; whereas the Hopkinson bar is used for experiments at strain rates in the range from 10^2 to 10^4 s^{-1} . Polymeric foams have thus been mechanically characterized mostly at low strain rates (up to 10^{-1} s^{-1}) or high strain rates (from 10^2 to 10^4 s^{-1}) [2–6]. By contrast, the mechanical response of the polymeric foams in the strain rate range from 10^{-1} to 10^2 s^{-1} , called intermediate strain rates, has been less studied because of difficulties in experimental techniques. Recently intermediate-rate experimental techniques have been gained attention [2, 3, 6–9], making it possible to obtain a complete stress–strain description in each order of strain rates from quasi-static to dynamic loading conditions. However, more attention still needs to be paid to obtain valid and accurate data particularly for low-density foam materials. When the foam materials have a low density, the strength and stiffness are so low that more challenges to obtain valid data are encountered in both quasi-static and dynamic experiments. For example, when characterizing a low-density foam material, the specimen deformation may not be uniform even in a quasi-static experiment [10]. A compaction front propagated through the sample during axial compression. This front divided the sample into packed and unpacked regions, making the test invalid for material property characterization. In a split Hopkinson pressure bar (SHPB) experiment, the non-uniform deformation becomes worse [10]. Therefore, efforts are required to achieve a uniform deformation in a low-density foam

B. Song · W. Chen (✉)
School of Aeronautics and Astronautics and School of Materials Engineering, Purdue University, 315 N Grant Street,
West Lafayette, IN 47907-2023, USA
e-mail: songb@purdue.edu

W.-Y. Lu
Sandia National Laboratories, Livermore, CA 94551-0969, USA

specimen. Recently, we have developed experimental techniques to meet these challenges, as documented in Refs. [11–14]. Employing modifications in both MTS and SHPB experiments, the foam specimen can be uniformly deformed at constant strain rates within a certain range [11–14].

In this study, we conducted compressive characterization of a low-density epoxy foam at various low, intermediate, and high strain rates. The stress–strain curves for the epoxy foam were obtained at the strain rates from 0.05 s^{-1} to $2,700\text{ s}^{-1}$ and the strain rate effects on the compressive response in this strain rate range were determined.

Material and specimen

In this study, the epoxy foam material, which was provided by Sandia National Laboratories, Livermore, CA, had a density of $0.12 \times 10^3\text{ kg/m}^3$. This removable epoxy foam which is designed to be cast in molding applications has properties comparable to conventional epoxy foam encapsulants, but can be removed with mild solvent at $90\text{ }^\circ\text{C}$ to allow for recovery of potted components when used as a potting material [15]. Figure 1 is a scanning electron micrograph that shows the microstructures of this epoxy foam. The epoxy foam has a closed-cell structure with an average cell size of $\sim 200\text{ }\mu\text{m}$.

The removable epoxy foam specimens had a diameter of 13.80 mm and a thickness of 2.70 mm. Such a thin specimen is necessary to achieve early uniform states in both stress and deformation in dynamic experiments [11, 12]. The foam specimens with a common dimension for experiments at all strain rates can eliminate specimen size effects and make the strain rate as the only variable to study strain rate effects.

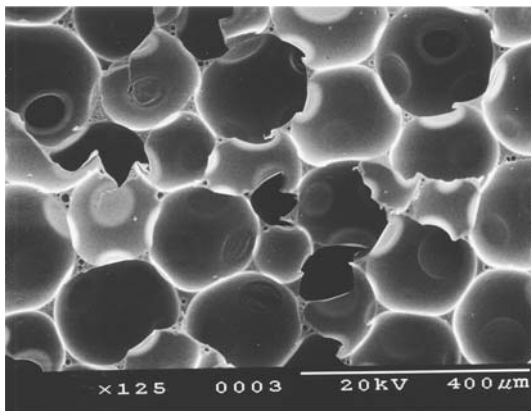


Fig. 1 Micrograph of the expandable epoxy foam

Experimental procedure

An MTS-810 materials testing machine was employed to conduct the compressive experiments at the strain rates from 0.05 s^{-1} to 35 s^{-1} . We used two specimen gripping systems of the MTS machine which are schematically shown in Fig. 2. Both configurations consist of two 19.05-mm-diameter steel bars as compressive grips. The only difference between the gripping systems is that we employed two quartz crystal force transducers at the ends of the bars for the experiments at 35 s^{-1} , as shown in Fig. 2b. The bars are held and guided with an alignment frame. This gripping system maintains a precise alignment during compression. Furthermore, the specimen gripping configuration in the MTS is the same as that in dynamic SHPB experiments that is described later, leaving strain rate as the only variable in the test conditions from quasi-static to dynamic experiments. The strain rate was varied through the control of hydraulic actuator moving velocity in displacement control mode (fixed crosshead velocity). The linear variable displacement transducer (LVDT) and load cell in the MTS machine were used to measure the end

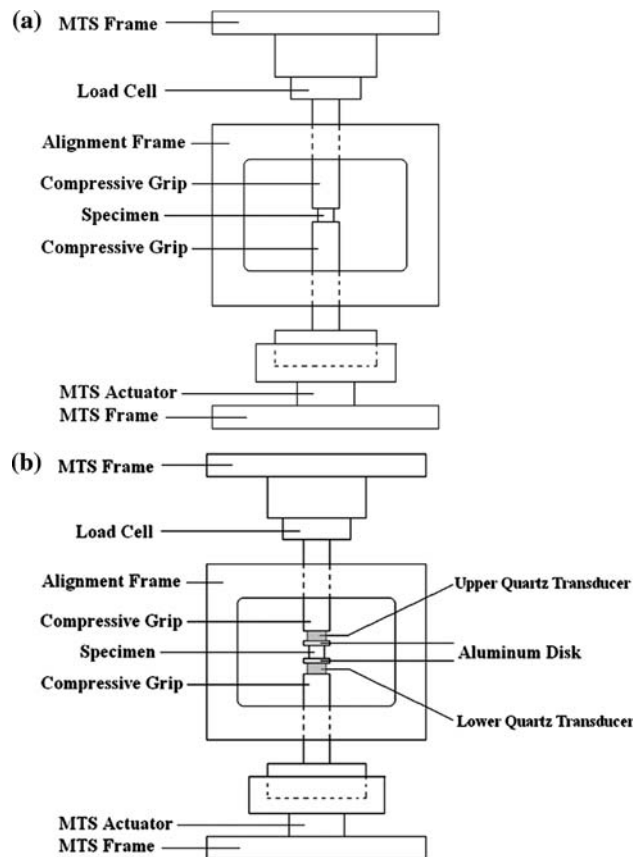


Fig. 2 Schematics of the regular and modified MTS gripping system with quartz transducers. (a) regular MTS gripping system; (b) modified MTS gripping system

displacement and force histories in the specimen, respectively.

When the speed of the actuator is slow such that the strain rate in the expandable epoxy foam specimen is less than 10^1 s^{-1} , the system in Fig. 2a has sufficient frequency response to obtain accurate stress–strain data for the foam materials. However, when the actuator moves faster, say 92 mm/s that corresponds to the engineering strain rate of 35 s^{-1} , the stress–wave propagation inside the load cell on the MTS machine and the check of uniform specimen deformation need to be concerned. The two force transducers that were placed at the ends of the guided steel bars near the specimen, as shown in Fig. 2b, had sufficient high frequency response and accuracy for the experiments at this speed. The 22-kN capacity force transducers, which were manufactured by Kistler, had a sensitivity of $\sim 12.4 \text{ pC/N}$. The signals from the force transducers were recorded with a Tektronix TDS 3000 digital oscilloscope through Kistler 5010B charge amplifiers. The force transducers were used to directly record the force histories at both ends of the specimen to check the stress equilibrium process during the experiment. Figure 3 shows the typical LVDT and force histories obtained with the MTS load cell and the force transducers in such an experiment on the epoxy foam specimen. The oscillations in the output signal from the load cell in Fig. 3 were caused by the wave propagation in the MTS system, in particular, in the load cell itself, indicating that the load cell did not provide sufficient frequency response for the test at this actuator speed. The structural response of the testing system is mixed with the specimen material response if the signal from the load cell is used for data reduction. However, the quartz crystal force transducers exhibit the capability to accurately record the force histories in specimen.

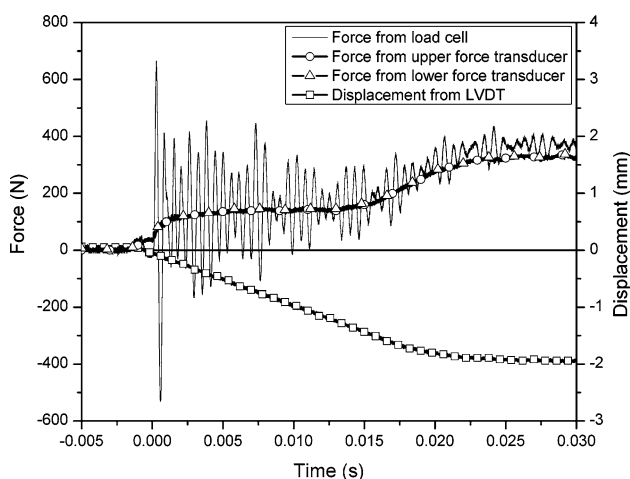


Fig. 3 Typical records from the load cell, quartz transducers, and the LVDT on the modified MTS

Moreover, the overlapping of the signals from both quartz crystal transducers implies that the specimen was in a state of stress equilibrium such that the resultant stress–strain curve is valid. This strain-rate level (35 s^{-1}) is near the capacity limit of the MTS machine for the epoxy foam specimen studied in this research.

Compressive experiments at higher strain rates were performed with a modified SHPB apparatus, the schematic of which is shown in Fig. 4. Besides the standard components in a conventional SHPB (a gas gun, a striker, an incident bar, a transmission bar, a momentum absorption device, and a data acquisition system), a pulse shaper at the impact end of the incident bar and two quartz crystal force transducers at both specimen ends were employed in the modified SHPB (Fig. 4), which are necessary for testing soft materials [11, 13]. The function of a pulse-shaper is to achieve dynamic stress equilibrium and constant strain-rate deformation in specimen as quickly as possible [11, 13]. Through varying material and dimensions of the pulse shaper as well as the impact velocity of striker, the profile of the incident pulse is precisely controlled such that the specimen deforms at a constant strain rate under dynamic stress equilibrium. Quartz-crystal force transducers attached to the bar ends near the soft specimen were used to directly record the axial load histories on the front and back surfaces of the specimen for the purposes of monitoring the stress equilibrium in specimens during experiments, which are similar to those in the modified MTS (Fig. 2b). The output signals from the quartz crystals were recorded using a high-speed digital oscilloscope (Tektronix TDS 3000) through charge amplifiers (Kistler 5010B).

When the desired strain rate is low in a SHPB experiment, the duration of loading pulse becomes long in order to deform the specimen to a sufficient strain. To record such a long loading pulse at relatively low strain rates, long incident and transmission bars are desired. In this study, the 19.05-mm-diameter aluminum alloy incident and transmission bars had the lengths of 3,658 mm and 2,134 mm, respectively. However, it is noted that the bars are still not long enough to fully record the long loading pulses without overlapping. We attached semi-conductor strain gages near the impact end of the incident bar to record the relatively-low-amplitude incident and reflected pulses. This modification can record a loading duration nearly twice as long as by a conventional method, without superposition between the incident and reflected pulses. However, it inevitably leads to overlapping of the reflected pulse with the signal that is reflected back into the incident bar at the impact end. However, we have properly recovered the needed information from such records [9, 14]. Figure 5 shows a typical oscilloscope record from such a pulse-shaped experiment. It has been demonstrated that the stress in specimen can be dynamically equilibrated through proper pulse shaping

Fig. 4 A schematic of the modified SHPB

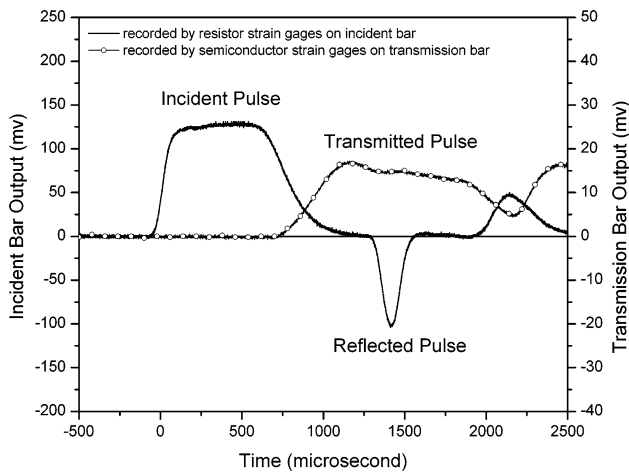
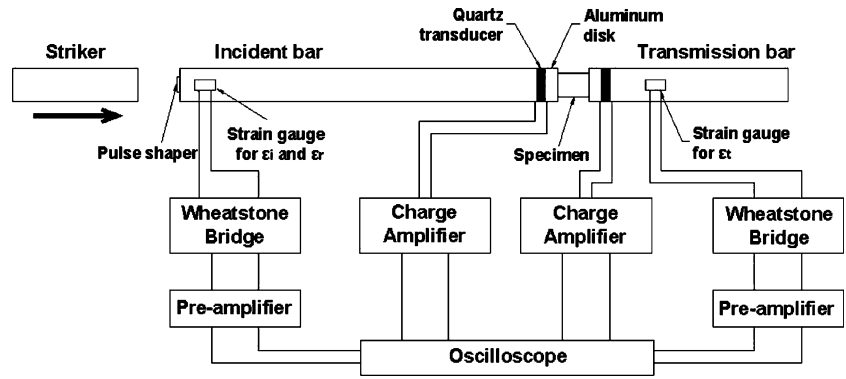


Fig. 5 A typical set of incident, reflected, and transmitted signals obtained from a SHPB experiment

techniques [11, 13]. The triangle-like reflected pulse in Fig. 5 indicates the result of such overlapping, from which we recovered the entire reflected through the methods introduced in Refs. [9, 14]. After the reflected pulse is recovered, the strain rate, strain and stress in specimen can be calculated through standard Hopkinson bar data reduction equations when dynamic stress equilibrium is satisfied,

$$\dot{\varepsilon}_r(t) = -2 \frac{C_0}{L_s} \varepsilon_r(t) \tag{1}$$

$$\varepsilon_r(t) = -2 \frac{C_0}{L_s} \int_0^t \varepsilon_r(t) dt \tag{2}$$

$$\sigma(t) = \frac{A_0}{A_s} E_0 \varepsilon_i(t) \tag{3}$$

where $\varepsilon_i(t)$, and $\varepsilon_r(t)$ are incident, reflected, and transmitted strain histories, respectively; A_0 is the cross-sectional area of the bars; E_0 and C_0 are Young’s modulus and elastic wave speed in the bar material, respectively; A_s and L_s are

initial cross-sectional area and length of the specimen, respectively. Figure 6 shows the recorded and recovered strain-rate histories from such an experiment, as well as strain history in specimen which were calculated with Eqs. (1) and (2). The plateau in the strain rate history and the linearity in the strain history in Fig. 6 indicate the constant strain-rate deformation in the specimen.

The usage of semi-conductor strain gages at the impact end of the incident bar was applied to experiments at the strain rates of 190 s^{-1} , 530 s^{-1} , and $1,150 \text{ s}^{-1}$. The compression experiments at the strain rate of $2,700 \text{ s}^{-1}$ followed the regular pulse-shaped Hopkinson bar experiments for the foam materials, where a pair of strain gages were mounted in the middle of the incident bar to record the incident and reflected pulses that were not overlapped each other at all.

Experimental results

The stress–strain curves for the epoxy foam at various strain rates from 0.05 s^{-1} to $2,700 \text{ s}^{-1}$ are summarized in

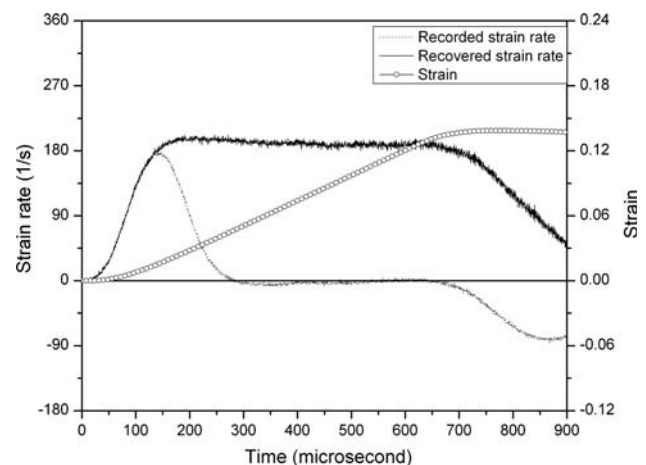


Fig. 6 Recorded and recovered strain-rate and strain histories in the specimen

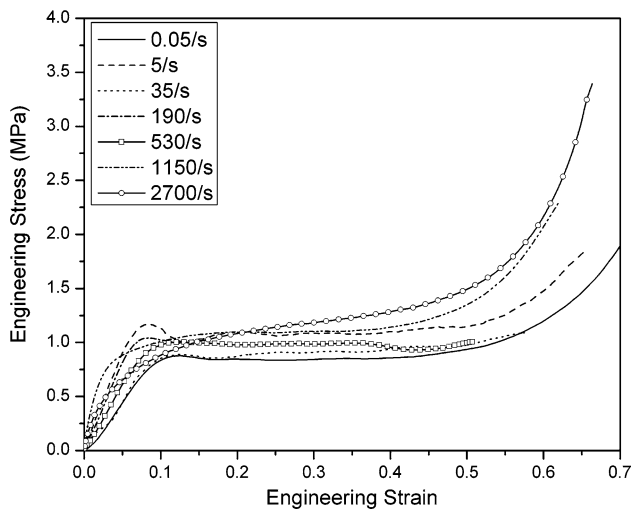


Fig. 7 Compressive stress–strain curves at various strain rates

Fig. 7. Figure 7 shows the mean of stress–strain curves at each strain rate obtained from repeatable experiments, which exhibit a typical stress–strain response for regular foam materials: initial linear elastic response followed by a plastic plateau and a densification [16].

There are two distinctive features that can be observed in Fig. 7. The first is that the stress–strain curves are provided for every strain-rate decade from quasi-static to dynamic without any gap in between. The second is that the stress–strain curves are extended to large strains (>50%) except for the curve obtained at 190 s^{-1} . Such complete sets of rate-dependent stress–strain data are not commonly seen in literature.

Due to distribution of cell size and structure in the thin specimens, the data exhibit scattering. However, we can still observe the trends in strain rate effects on the foam. The modulus of elasticity, cell-collapse strength, and plateau stress all increase with increasing strain rate. In the range of strain rate studied in this research, the modulus of elasticity varies between 10 MPa and 30 MPa. The cell-collapse stress varies between 0.88 MPa and 1.17 MPa, whereas the plateau stress varies between 0.84 MPa and 1.14 MPa. Figure 8 shows the detailed strain-rate dependencies of the modulus of elasticity and the cell-collapse stress for the epoxy foam material. It is noted that the modulus of elasticity obtained at the strain rate of $1,150\text{ s}^{-1}$ or higher is not accurate because the foam specimen has not achieved the desired strain rate before the specimen is collapsed [17, 18]. For example, the strain rate did not reach the desired value of $2,700\text{ s}^{-1}$ when the cell structures started to collapse in the mechanical testing at the eventual strain rate of $2,700\text{ s}^{-1}$. Therefore, we can only reliably examine the strain-rate effects on the modulus of elasticity in the strain-rate range below $1,150\text{ s}^{-1}$ and on

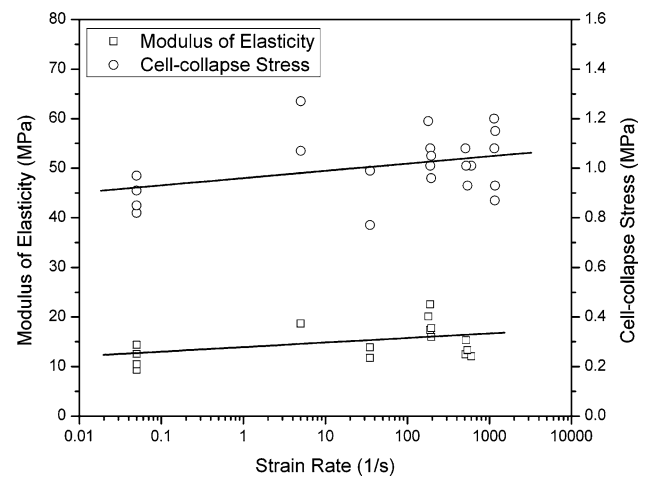


Fig. 8 Strain-rate effects of the modulus of elasticity and early cell-collapse stress

the cell-collapse stress below $2,700\text{ s}^{-1}$. Both modulus of elasticity and cell-collapse stress are found to linearly increase with the increasing logarithm of strain rate, as shown in Fig. 8.

Conclusions

A modified MTS and SHPB were employed for mechanical characterization of a low-density epoxy foam at various strain rates in this study. Beside typical usage of the MTS and SHPB for low- and high-rate testing, both MTS and SHPB were modified for intermediate strain-rate experiments. The compressive stress–strain curves of the epoxy foam were determined at a variety of strain rate from 0.05 s^{-1} to $2,700\text{ s}^{-1}$ without any gap in the intermediate-rate range. The experimental results show that the epoxy foam exhibits strain rate effects on both the modulus of elasticity and cell-collapse stress.

Acknowledgements This work was supported by Sandia National Laboratories, Livermore, CA. Sandia is a multiprogram laboratory operated by Sandia Corporation, a Lockheed Martin Company, for the United States Department of Energy under Contract DE-AC04-94AL8500.

References

1. Kolsky H (1949) Proc Phys Soc London B62:676
2. Rinde JA, Hoge KG (1971) J Appl Polymer Sci 15:1377
3. Zhao H (1997) Polym Test 16:507
4. Chen W, Lu F, Winfree N (2002) Exp Mech 42:65
5. Chakravarty U, Mahfuz H, Saha M, Jeelani S (2003) Acta Mater 51:1469
6. Ouellet S, Cronin D, Worswick M (2006) Polym Test 25:731
7. Zhao H, Gary G (1997) J Mech Phys Solids 45:1185
8. Zhao H, Gary G (2002) Int J Vehicle Des 30:135

9. Song B, Chen W, Lu W-Y (2006) *Int J Mech Sci* (in press)
10. Song B, Forrestal MJ, Chen W (2006) *Exp Mech* 46:127
11. Chen W, Lu F, Frew DJ, Forrestal MJ (2002) *Trans ASME J Appl Mech* 69:214
12. Song B, Chen W (2004) *Exp Mech* 44:300
13. Song B, Chen W, Jiang X (2005) *Int J Vehicle Design* 37:185
14. Chen WW, Song B (2005) In: *Experiments in Automotive Engineering—Optical Techniques*, SAE Trans, 2005 SAE World Congress, April 11–14, 2005, Detroit, MI, USA
15. McElhanon JR, Russick EM, Wheeler DR, Loy DA, Aubert JH (2002) *J Appl Polym Sci* 85:1496
16. Gibson LJ, Ashby MF (1999) *Cellular solids, structure and properties*, 2nd edn. Cambridge
17. Song B, Chen WW, Dou S, Winfree NA, Kang JH (2005) *Int J Impact Eng* 31:509
18. Pan Y, Chen W, Song B (2005) *Exp Mech* 45:440